IC 9304

Smoke, Carbon Monoxide, and Hydrogen Chloride Production From the Pyrolysis of Conveyor Belting and Brattice Cloth

By Margaret R. Egan

UNITED STATES DEPARTMENT OF THE INTERIOR

Information Circular 9304

Smoke, Carbon Monoxide, and Hydrogen Chloride Production From the Pyrolysis of Conveyor Belting and Brattice Cloth

By Margaret R. Egan

CONTENTS

UNIT OF MEASURE ABBREVIATIONS USED IN THIS REPORT

°C	degree Celsius	m^2	square meter
cm	centimeter	m^3/s	cubic meter per second
g/cm^3	gram per cubic centimeter	mg/m^3	milligram per cubic meter
$g/(m^3 \cdot ppm)$	gram per cubic meter times part per million	min	minute
g/s	gram per second	μm	micrometer
$g/(m^2 \cdot s)$	gram per square meter times second	p/cm^3	particle per cubic centimeter
h	hour	pct	percent
m	meter	ppm	part per million
m^{-1}	reciprocal meter	V	volt

SMOKE, CARBON MONOXIDE, AND HYDROGEN CHLORIDE PRODUCTION FROM THE PYROLYSIS OF CONVEYOR BELTING AND BRATTICE CLOTH

By Margaret R. Egan[1]

ABSTRACT

In an underground mine fire, a toxic mixture of combustion product gases and particulate matter is transported by the ventilating system endangering everyone downstream. To determine the magnitude of the problem that these toxic combustion products pose, the U.S. Bureau of Mines is investigating the combustion products of typical materials found in underground mines. The total toxicity of the combustion products depends upon the evolving gas species and particulate matter, the amount of material involved, and the ventilation rate. In a simulated mine environment, the products from smoldering polyvinyl chloride (PVC) brattice and conveyor belting were analyzed for gas concentrations and smoke characteristics. The primary toxic gases are hydrogen chloride (HCl) and carbon monoxide (CO). Smoldering conveyor belts are more detectable than smoldering PVC brattice cloths. These results, combined with previous analyses, are used to estimate relative toxicities, product levels, and detectability of smoldering mine combustibles.

[1]Research chemist, Pittsburgh Research Center, U.S. Bureau of Mines, Pittsburgh, PA.

INTRODUCTION

In a fire, smoke is the most important factor affecting life and property. It may be defined as the airborne products evolved when organic materials smolder or burn. It can obscure the route to safety by irritating the eyes and respiratory tract and can cause injury or death by inhalation. Smoke is not only the first sign of an impending disaster but also it can trigger an alarm saving lives and property. Developing sensitive and effective smoke detectors has been a challenge accepted by the U.S. Bureau of Mines.

Brattice cloth is used as a space divider or temporary partition installed to direct the airflow. Brattices were formerly made of untreated jute, but nylon-reinforced plastics or similar materials are more commonly used today. Most conveyor belts used in mines today contain a halogenated base polymer or are treated with a halogenated fire retardant.

Since the introduction of synthetic components, the fire problem has taken on yet another dimension—that of the possible production of additional toxic gases. In ventilated passageways, the risks from fires are compounded because the toxic gases and smoke can be transported throughout the mine endangering people far removed from the actual flames. The Bureau uses an intermediate-scale fire tunnel at the Pittsburgh Research Center to simulate a mine environment.

This report focuses on the smoldering combustion, its detection, and relative toxicity. Once the emission products of combustible materials are known, more efficient detection, fire-suppression, and rescue equipment can be designed to improve health and safety conditions in underground mines.

The objectives of this study were to analyze the gas concentrations and particulate characteristics of smoldering brattice cloths and conveyor belting. The thermal decomposition results presented in this report, together with previous analyses of data for wood, transformer fluid, coal, conveyor belting, and ventilation ducting $(1-5)$[2] form a data base by which future findings of other mine combustibles can be compared.

EXPERIMENTAL EQUIPMENT

INTERMEDIATE-SCALE FIRE TUNNEL

A schematic of the Bureau's intermediate-scale fire tunnel with its data-acquisition system is shown in figure 1. A bidirectional flow probe (6) with a pressure transducer was used to determine velocity. The airflow was produced by the exterior exhaust fan and was detected by the flow probe centered in the air-intake cylinder.

Before each experiment, background readings were obtained after the material was positioned and the exhaust fan was started. Every minute throughout the experiment, the readings from each channel are scanned, stored, and displayed. After the experiment was completed, the data were plotted.

GAS ANALYZERS

The CO analyzer measures accurately within 1 pct of the range or ± 1 ppm. The carbon dioxide (CO_2) analyzer measures accurately within 1 pct of the range or ± 25 ppm. The HCl analyzer has a sensitivity of 0.2 ppm. These analyzers were calibrated at the beginning of each experiment.

SMOKE MONITORS

The particle number concentration (N_o) was obtained with a condensation nuclei monitor (CNM), manufactured by Environment One Corp.,[3] Schenectady, NY. This monitor uses a cloud chamber to measure the concentration of submicrometer airborne particles (p). The particulate cloud attenuates a light beam which ultimately produces a measurable electrical signal. The accuracy is stated as ± 20 pct of a point above 30 pct of scale within the linear range from 3,000 to 300,000 p/cm^3. Therefore, in these experiments, the calculated error could have been as great as $\pm 18,000$ p/cm^3.

The particle mass concentration (M_o) was obtained by a tapered-element oscillating microbalance (TEOM) developed by Rupprecht & Patashnick Co., Inc., Voorheesville, NY (7). It measures the mass directly by depositing the particles on a filter attached to an oscillating tapered element. The oscillating frequency of the tapered element decreases as the deposited mass increases. The apparatus is capable of measuring the particulate concentration with a better than 5 pct accuracy at the level used. According to the manufacturer, the filter collects at least 50 pct of all particles with a volume mean diameter of 0.05 μm, with increasing collection efficiency as the diameter increases. Actual data obtained by the Bureau using particles of volume mean diameter equal to 0.048 μm indicated a collection efficiency closer to 90 pct.

---

[2]Italic numbers in parentheses refer to items in the list of references preceding the appendix at the end of this report.

[3]Reference to specific products does not imply endorsement by the U.S. Bureau of Mines.
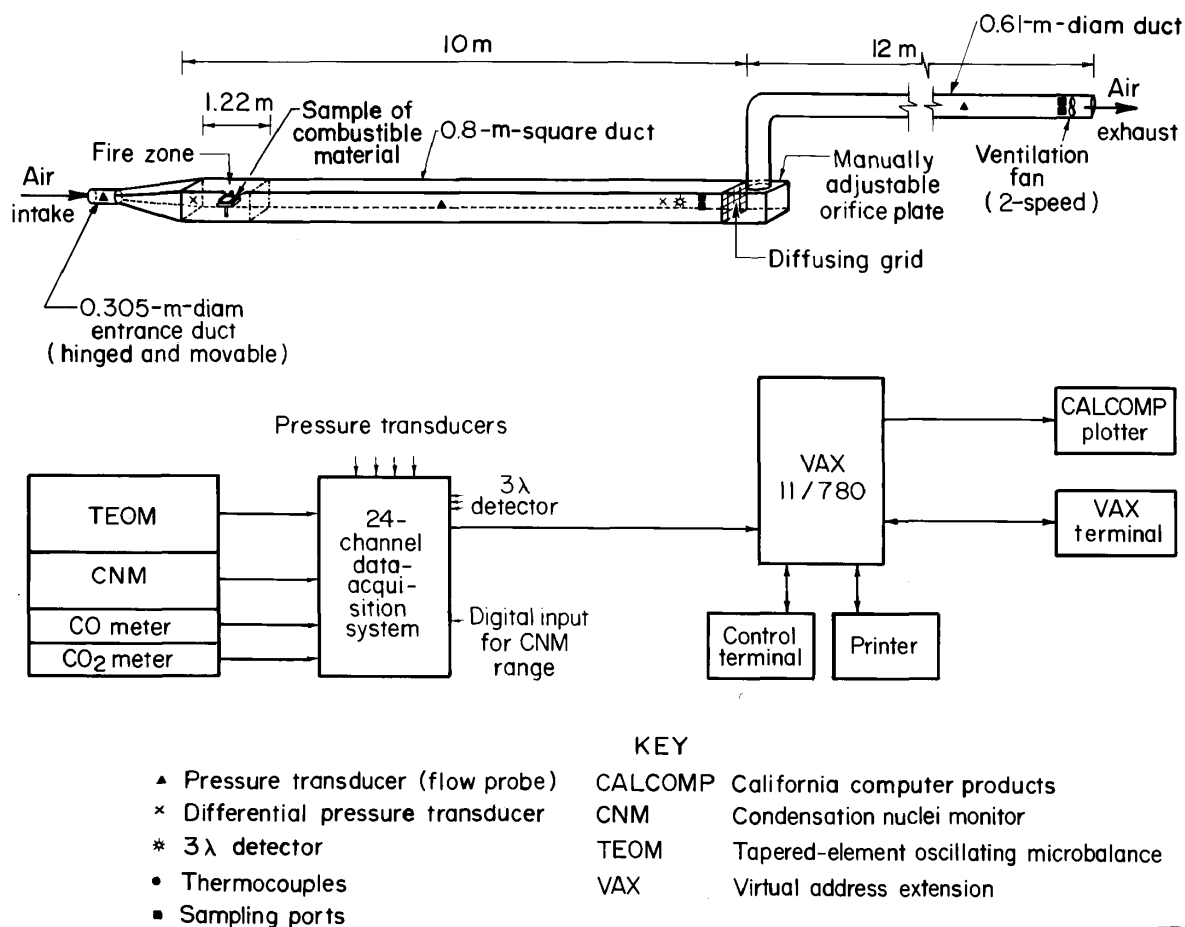
Figure 1.—Schematic of intermediate-scale tunnel (top) and data-acquisition system (bottom).

KEY

▲ Pressure transducer (flow probe)   CALCOMP   California computer products
× Differential pressure transducer   CNM   Condensation nuclei monitor
✳ 3λ detector   TEOM   Tapered-element oscillating microbalance
● Thermocouples   VAX   Virtual address extension
■ Sampling ports

Since the diameter of average mass is calculated from the mass and number concentrations, its accuracy was dependent upon the precision of the TEOM and CNM. Considering the error estimates of the mass and number concentrations, the diameter of average mass could vary by ±0.05 μm.

A three-wavelength light-transmission technique (8) developed by the Bureau was used to measure particle size and smoke obscuration. White light was transmitted through the smoke cloud to the detector. The beam was split into three parts, and each passed through an interference filter centered at wavelengths of either 0.45, 0.63, or 1.00 μm. Each photodiode output was amplified and recorded.

MATERIALS AND TEST PROCEDURES

Table 1 lists the materials studied with their chlorine content. Flaming combustion emissions of some of the same conveyor belts were studied using a natural gas burner as the ignition source. The results of these studies have been reported in reference 4.

Conveyor belts: A 23- by 30-cm section of each belt was tested in duplicate or triplicate depending on the amount of belting available. The belts were classified according to covering. They included six different PVC belts, one styrene-butadiene rubber (SBR) belt, and one

neoprene (NP) belt. Three electric strip heaters were clamped on top of each belt sample. The power was set at 150 V for the 30 min duration of the experiment.

Brattice cloth: Nine different PVC brattice cloths and one sample of jute brattice (treated with fire retardant) were tested in duplicate. A double thickness of brattice measuring 23- by 30-cm was placed on a wire mesh which rested on three strip heaters. The power was set at 100 V for 5 min and increased to 175 V for the remaining 25 min of the experiment.

The pyrolysis of the conveyor belting and brattice cloth did not result in flaming combustion. The combustion emissions were designated initial and steady state. After the strip heaters were turned on, the initial production occurred on average between the 9th and 19th min for the conveyor belting and the 13th and 16th min for brattice cloth. These results were usually the peak emission levels. After this period, the steady-state production occurred between the 21st and 30th min for conveyor belting and the 22nd and 30th min for brattice cloth. The ventilation rate (V_oA_o) throughout all the experiments averaged 0.16 m^3/s.

Table 1.—Materials analyzed

Material	Description	Chlorine, pct	Material	Description	Chlorine, pct
	BRATTICE CLOTH			CONVEYOR BELTING	
A	Polymer component is PVC resin	22.99	P1	Polymer component is PVC resin. .	23.00
B	..do	29.29	P1A ...	..do	21.00
C	..do	37.99	P2	..do	11.13
D	..do	40.39	P3	..do	18.34
E	..do	34.59	P4	..do	4.40
F	..do	37.59	P8	..do	15.20
G	..do	26.59	SBR ...	Polystyrene-butadiene rubber with chlorinated additives.	5.38
H	..do	28.99			
I	..do	27.53	NP	Polymer component is neoprene rubber.	12.86
Jute ...	Jute burlap with chlorinated additives	7.27			

CALCULATIONS

It is necessary to measure certain parameters to compare the combustion products, hazard potential, and detectability of various fuels. The measurements include gas concentrations, smoke particle M_o and N_o, and V_oA_o. Other combustion properties can be calculated once these values are known.

PRODUCT GENERATION RATES

The generation rate, $\dot{G}_X$, of a product is related to its measured concentration and V_oA_o by the general expression

$$\dot{G}_X = M_X (V_oA_o) (\Delta X), \qquad (1)$$

where, for gases M_{CO_2} = 1.97 × 10^{-3} g/(m³·ppm),

M_{CO} = 1.25 × 10^{-3} g/(m³·ppm),

M_{HCl} = 1.63 × 10^{-3} g/(m³·ppm),

V_oA_o = ventilation rate, m³/s,

and ΔX = measured quantity of a given gas.

To determine the amount of toxic gas generated from the combustion of a specific area of a sample, the following expression can be used

$$\dot{G}'_X = \dot{G}_X/A_H, \qquad (2)$$

where A_H is area of the strip heaters, 0.02 m². The decomposition of the conveyor belts occurred only where the belt came into direct contact with the strip heaters. By contrast, the entire sample of PVC brattice cloth was destroyed. At any one time, this area measured between 0.02 m² (the area of the strip heaters) and 0.07 m² (the entire sample area). For the steady-state stage calculations, an average area of 0.045 m² was chosen to represent the involved area of the brattice sample.

The concentrations of toxic gas can be predicted for a certain area and V_oA_o by the following expression

$$\Delta X = \frac{\dot{G}'_X}{M_X} \left[\frac{A_S}{V_oA_o} \right] \qquad (3)$$

where A_S is heated area of the sample, and M_X is density of a given gas.

To estimate the toxicity of the CO and HCl emissions, two established levels will be considered. The first level is the threshold limit value (TLV), which represents the maximum average exposure that can be tolerated for an 8-h period without suffering any adverse effects. The TLV for CO is 50 ppm and for HCl is 5 ppm (9). The second level is the immediately dangerous to life and health (IDLH), which represents the level at which severe health effects and possibly death could occur. The IDLH for CO is 1,500 ppm (10) and for HCl is 100 ppm (11). Assuming that the toxicities of combined CO and HCl are additive (12), then if the sum of the following fractions

$$\frac{\Delta CO}{50\,ppm} + \frac{\Delta HCl}{5\,ppm} \leq 1, \tag{4}$$

the TLV of the mixture has not been exceeded (13). Similarly, when

$$\frac{\Delta CO}{1,500\,ppm} + \frac{\Delta HCl}{100\,ppm} \leq 1, \tag{5}$$

the IDLH level has not been exceeded, and the toxicity is not life-threatening. Then, when the following expression

$$\frac{A_S}{V_o A_o} \leq \frac{1}{\dfrac{\dot{G}'_{CO}}{50\,M_{CO}} + \dfrac{\dot{G}'_{HCl}}{5\,M_{HCl}}} \tag{6}$$

is satisfied, the combined toxicity is within the TLV. Similarly, when the following expression is satisfied, the combined toxicity exceeds or is equal to the IDLH level.

$$\frac{A_S}{V_o A_o} \geq \frac{1}{\dfrac{\dot{G}'_{CO}}{1,500\,M_{CO}} + \dfrac{\dot{G}'_{HCl}}{100\,M_{HCl}}} . \tag{7}$$

Early fire detection can minimize the toxic and irritating effects of combustion emissions and maximize the chances of escape or rescue. However, a balance must be reached between an alarm threshold that is low enough to be effective and still reliable. The minimum requirements for CO sensor alarm thresholds, CO_A, can be calculated by using the A_S-$V_o A_o$ ratio for TLV from equation 6 in the following expression,

$$CO_A = \frac{\dot{G}'_{CO}}{M_{CO}} \left[\frac{A_S}{V_o A_o} \right]. \tag{8}$$

An evaluation of combustion toxicity and detectability would not be complete without considering the smoke intensity and particle size.

SMOKE PARTICLE DIAMETERS

Measurements of both M_o and N_o of the smoke can be used to calculate the average size of the smoke particles, using the expression

$$\frac{\pi d_m^3}{6} (\rho_p) N_o = 1 \times 10^3 M_o, \tag{9}$$

where d_m = diameter of a particle of average mass, μm,

ρ_p = individual particle density, g/cm^3,

N_o = number concentration, p/cm^3,

and M_o = mass concentration, mg/m^3.

If the value of $\rho_p = 1.4$ g/cm^3, then the d_m can be calculated in micrometers from

$$d_m = 11.09 \left[\frac{M_o}{N_o} \right]^{1/3} . \tag{10}$$

When the three-wavelength smoke detector is used, the transmission of the light, T, through the smoke can be calculated for each wavelength. The extinction-coefficient ratio can be calculated for each pair of wavelengths, λ, from the following log-transmission ratios:

$$\frac{\ln T_{\lambda=1.00}}{\ln T_{\lambda=0.63}}, \qquad \frac{\ln T_{\lambda=1.00}}{\ln T_{\lambda=0.45}}, \qquad or \qquad \frac{\ln T_{\lambda=0.63}}{\ln T_{\lambda=0.45}} .$$

When these extinction coefficients and the curve in figure 11 of reference 8 are used, the surface mean particle size, d_{32}, can be determined. (Calculation of the extinction-coefficient curves assumes spherical particles with an estimated refractive index.) The T must be less than 85 pct before reliable particle sizes can be calculated using this technique.

SMOKE INTENSITY PARAMETERS

Another important factor of the particulate phase of smoke is visual obscuration. Smoke concentration is most often expressed in terms of optical density (OD) in reciprocal meters. This characteristic provides a measure of fire hazard, in that escape and rescue depend on visibility. It is related to T by the following expression:

$$OD = \frac{-1}{\ell} (\ln T), \tag{11}$$

where ℓ = path length, m.

Most smoke detectors are triggered at an OD of 0.1 m⁻¹ or less. The probability of escape and rescue is reduced significantly once the critical level of smoke (OD = 0.5 m⁻¹) has accumulated (14).[4] The minimum requirements for smoke sensor alarm thresholds, OD_A, can be determined in a similar manner to CO_A (equation 6) by the following expression

$$OD_A = \frac{\dot{G}'_{CO}}{M_{CO}}\left(\frac{OD}{CO}\right)\left(\frac{A_S}{V_oA_o}\right). \qquad (12)$$

Smoke density may be defined as the degree of light obscuration produced by the smoke from the burning material under given conditions of combustion. Some other factors influencing obscuration include the number, size, and refractive index of the particles and light frequency. The smoke obscuration is the percentage of light absorbed by the smoke or 100 pct of the light minus the percent T. It is calculated using the following equation:

$$Obscuration = 100(1 - T). \qquad (13)$$

The obscuration values presented in this report are an average of the attenuation of the beam of light at two wavelengths in the visible range, 0.45 and 0.63 μm.

RESULTS AND DISCUSSION

Figure 2 shows the charred remnant of a PVC brattice after pyrolysis. At least two thirds of the brattice was consumed in the typical experiment. By contrast, the exterior of the conveyor belting was only scorched by the strip heaters with little damage to the interior fibers. The average PVC belt lost 14 pct of its mass while the NP belt lost 7 pct and the SBR belt lost only 3 pct. Table 2 lists the mass loss and steady-state temperature for each belt and brattice. A probe located above, but not touching the test sample was used to determine temperature. All the reported results are an average from all experiments for each belt and brattice. Figures 3, 4, and 5 illustrate the typical gas and smoke production as a function of time for PVC belt, P1, and PVC brattice, I.

GAS CONCENTRATIONS

These hydrocarbons were found in grab samples of the steady-state emissions of PVC brattices. They included: 8 ppm methane, <2 ppm ethane and ethylene, and <1 ppm propane and propylene. However, the concentrations of CO, CO_2, and HCl were continuously measured. These initial gas concentrations and ratios for each belt and brattice are listed in table 3. The same determinations for the steady-state stage are listed in table 4.

For all belts, the CO production remains fairly constant throughout the experiments. However, for brattice, the CO production decreases as the cloth is consumed. Figure 3 compares the production of CO for a typical PVC belt and brattice. The amount of material consumed must be considered when comparing the relative concentrations of CO produced. Initially, all brattices but A, F, G, and H produced CO above the detection level of 5 ppm.

Table 2.—Mass loss and steady-state temperature

Material	Δm, g	Δm, pct	Temp, °C
BRATTICE CLOTH			
A	25.5	43.1	330
B	57.8	44.9	407
C	42.7	48.4	344
D	37.5	45.2	296
E	46.2	47.0	281
F	9.7	40.9	220
G	29.1	39.8	266
H	18.2	36.4	289
I	26.6	42.7	219
Jute	ND	ND	ND
CONVEYOR BELTING			
P1	125.0	14.2	94
P1A	122.2	13.7	93
P2	142.2	12.8	77
P3	119.4	13.3	77
P4	118.3	13.0	127
P8	162.2	17.3	82
SBR	43.5	3.2	113
NP	61.3	6.9	214

ND   Not determined.

---

[4]Reference 14 quotes a value of OD = 0.218 m⁻¹ for the critical value determined from the expression OD = -1/ℓ log T. When the natural logarithm is used, as in equation 11, then OD = 2.303 × 0.218 = 0.5 m⁻¹, the value used in the text.
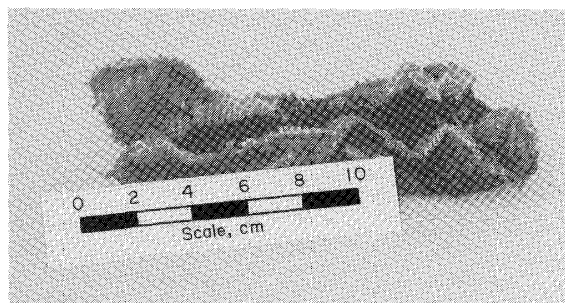

Figure 2.—Appearance of PVC brattice after pyrolysis.

Table 3.—Initial gas concentrations and ratios from smoldering brattice cloth and conveyor belting

Sample	CO, ppm	CO_2, ppm	Ratio, CO_2-CO	HCl, ppm	Ratio, HCl-CO
BRATTICE CLOTH					
A	4	19	4.4	31	7.0
B	12	86	6.0	36	2.9
C	17	18	1.1	69	4.5
D	5	34	6.5	70	14.4
E	13	70	5.3	18	1.4
F	2	34	13.8	10	4.3
G	4	23	5.1	37	7.6
H	2	32	15.4	11	5.2
I	7	23	3.4	16	2.2
Jute . . .	32	149	4.7	ND	ND
CONVEYOR BELTING					
P1	32	44	1.3	19	0.6
P1A . . .	42	49	1.2	15	.4
P2	32	39	1.2	13	.4
P3	17	24	1.4	24	1.4
P4	20	13	.6	12	.6
P8	41	15	.4	20	.5
SBR . . .	10	20	.5	5	.5
NP	12	24	1.4	17	1.4

ND   Not determined.

Table 4.—Steady-state gas concentrations and ratios from smoldering brattice cloth and conveyor belting

Sample	CO, ppm	CO_2, ppm	Ratio, CO_2-CO	HCl, ppm	Ratio, HCl-CO
BRATTICE CLOTH					
A	1	0	0.0	9	8.2
B	15	70	4.7	35	2.3
C	12	26	2.1	28	2.3
D	2	3	1.8	25	15.4
E	4	46	12.7	26	7.4
F	1	5	4.0	3	2.3
G	1	5	3.8	8	6.7
H	1	3	3.4	8	10.0
I	2	10	4.6	10	4.5
Jute . . .	7	69	9.9	ND	ND
CONVEYOR BELTING					
P1	34	61	1.8	11	0.3
P1A . . .	37	62	1.7	10	.3
P2	30	48	1.6	14	.5
P3	19	27	1.4	14	.7
P4	22	33	1.5	7	.3
P8	44	24	.6	12	.3
SBR . . .	10	14	1.5	3	.3
NP	12	30	2.5	12	1.0

ND   Not determined.

The CO_2 concentrations for the PVC and NP belts increased slightly from the initial stage to the steady-state stage. The SBR belt showed a slight decrease in CO_2 production. For PVC and jute brattice, the CO_2 concentrations decreased. However, jute brattice produced the highest concentration of CO_2 of all the materials. The CO_2-CO ratios in both stages were higher for brattices than for belts. During the steady state, incomplete oxidation produces less CO_2 lowering the CO_2-CO ratios of both belts and brattices.

The main toxic risk from the pyrolysis of PVC is HCl production. As little as 5 to 10 ppm can cause irritation to the mucous membranes (9). Some correlation between chlorine content and HCl production was found. For example, brattices with high chlorine content tend to emit high concentrations of HCl and conveyor belts with low chlorine content tend to emit low concentrations of HCl. For both brattice and belting, the HCl emissions are higher in the initial stage than the steady-state stage (fig. 4). The belts, at temperatures averaging less than 100° C, release HCl slowly showing an initial peak followed by a gently decreasing steady-state production of HCl. Most of the HCl is emitted as the polymeric material is being consumed in the initial stage. At this stage, the temperatures averaged 300° C.

The greatest ratio variation between the belts and brattices is seen in HCl-CO ratios. The brattices have high ratios averaging 6.5 in the initial stage and 5.5 in the steady-state stage. The PVC belts have much lower ratios averaging 0.6 in the initial stage and 0.4 in the steady-state stage.
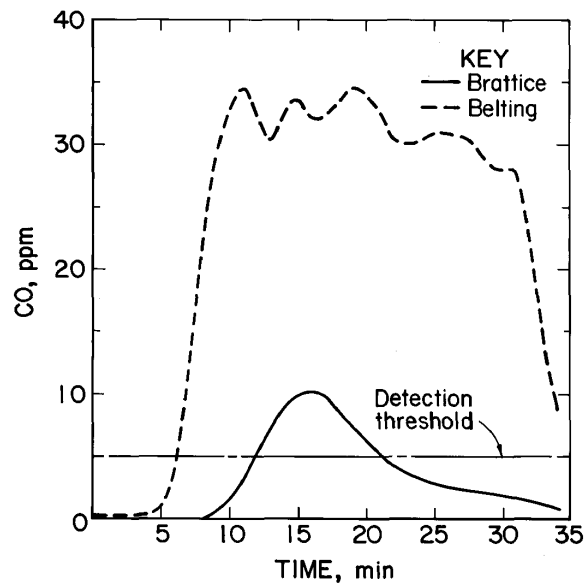

Figure 3.—Results of typical CO concentrations for PVC brattice and conveyor belting.
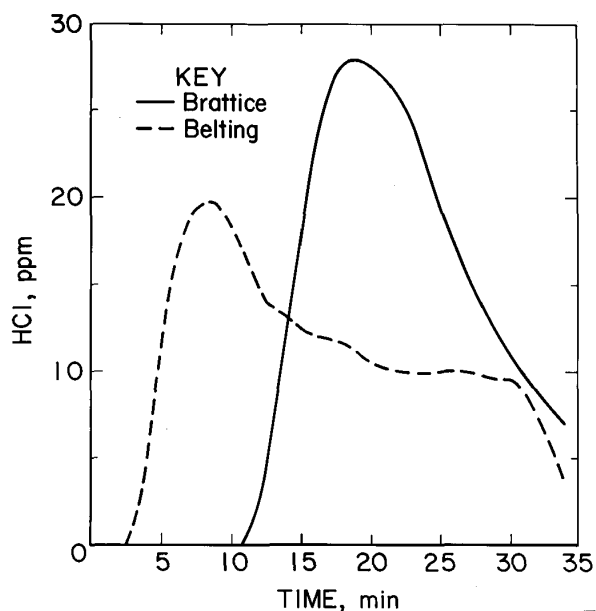
Figure 4.—Results of typical HCl concentrations for PVC brattice and conveyor belting.

Using the data in tables 5 and 6, equations 6 can be used to calculate the maximum A_S-V_oA_o ratio at which a safe-working environment exists. For example, brattice F with low CO and HCl production has an A_S-V_oA_o ratio of 8, whereas, belt P8 with high CO and HCl production has a ratio of 0.4. Low ratios would indicate a greater potential for dangerous conditions to exist because smaller amounts of sample or higher V_oA_o would be needed to keep the toxic levels below the TLV and IDLH levels. In these experiments, the actual A_S-V_oA_o ratio is 0.125 for conveyor belts (both stages) and brattices (initial stage only) and 0.281 for brattices (steady-state stage). Using these actual ratios, only brattice F and the SBR belt are in the safe region. Table 3 confirms that these samples have low combined CO and HCl emissions. Table 7 lists the maximum A_S-V_oA_o ratios to achieve the upper limit for the TLV and IDLH levels. When the calculated ratios exceed the actual ratios, a safe environment exits. Low ratios indicate potentially toxic levels as demonstrated by brattices C and D and belts P1A and P8 in the initial stage.

SMOKE CHARACTERISTICS

The smoke characteristics including N_o, M_o, particle size, obscuration, and OD for the initial stage of belts and brattices are listed in table 8. The same values for the steady-state stage are listed in table 9.

Many differences can be found between the smoke emissions of brattice and belting. The difference in M_o is the most noticeable property. It influences both the particle size and smoke obscuration. PVC belts with larger particles had higher M_o and obscured more light than the other belts and brattices. This occurred in both stages of combustion. Good agreement can be seen between the d_m and d_{32} that are measured independently. All the materials produced smoke above the OD detection level of 0.1 m^{-1} and all but jute produced smoke above the OD critical level of 0.5 m^{-1}. The profile of the OD curve (fig. 5) resembles the CO curve (fig. 3). The PVC belt produces steady smoke throughout the experiment while the PVC brattice produced more smoke in the initial stage.

Table 5.—Initial generation rates from smoldering brattice cloth and conveyor belting

Sample	$\dot{G}_{CO}$, 10^{-3} g/s	$\dot{G}_{CO_2}$, 10^{-3} g/s	$\dot{G}_{HCl}$, 10^{-3} g/s	$\dot{G}'_{CO}$, g/(m²·s)	$\dot{G}'_{HCl}$, g/(m²·s)
BRATTICE CLOTH					
A	0.9	6.3	8.2	0.04	0.41
B	2.5	27.0	9.3	.12	.47
C	3.4	5.7	18.5	.17	.93
D	1.1	11.1	19.3	.05	.96
E	2.6	21.4	4.7	.13	.24
F	.5	10.8	2.8	.02	.14
G	.9	7.3	8.5	.05	.43
H	.4	10.4	2.9	.02	.15
I	1.3	7.2	4.2	.07	.21
Jute ..	6.3	46.3	ND	.32	ND
CONVEYOR BELTING					
P1 ...	6.4	13.6	4.9	0.32	0.24
P1A ..	8.8	16.8	3.8	.44	.19
P2 ...	6.4	12.4	3.3	.32	.17
P3 ...	3.5	7.5	6.3	.18	.31
P4 ...	4.0	4.0	3.0	.20	.15
P8 ...	8.0	4.8	5.1	.40	.26
SBR ..	2.0	6.2	.2	.10	.06
NP ...	2.3	7.2	4.3	.12	.21

ND   Not determined.

Table 6.—Steady-state generation rates from smoldering brattice cloth and conveyor belting

Sample	$\dot{G}_{CO}$, 10^{-3} g/s	$\dot{G}_{CO_2}$, 10^{-3} g/s	$\dot{G}_{HCl}$, 10^{-3} g/s	$\dot{G}'_{CO}$, g/(m²·s)	$\dot{G}'_{HCl}$, g/(m²·s)
BRATTICE CLOTH					
A	0.2	0.0	2.5	0.01	0.05
B	2.9	21.4	8.9	.06	.20
C	2.3	8.3	7.5	.05	.17
D	.3	1.0	6.7	.01	.15
E	.7	13.5	6.5	.02	.14
F	.3	1.7	.7	.01	.01
G	.3	1.7	2.0	.01	.05
H	.2	.9	2.0	<.01	.04
I	.4	3.0	2.4	.01	.05
Jute ..	1.3	20.4	ND	.07	ND
CONVEYOR BELTING					
P1 ...	6.6	18.7	2.8	0.33	0.14
P1A ..	7.7	21.0	2.6	.38	.13
P2 ...	6.0	15.2	3.7	.30	.18
P3 ...	3.8	8.4	3.6	.19	.18
P4 ...	4.3	10.3	1.9	.22	.09
P8 ...	8.4	7.4	2.9	.42	.15
SBR ..	1.8	4.1	.7	.09	.04
NP ...	2.3	8.9	3.1	.12	.15

ND   Not determined.

Table 7.—A_s-$V_o A_o$ ratios for TLV and IDLH from initial and steady-state stages of smoldering brattice cloth and conveyor belting

Sample	Ratio, $(A_s\text{-}V_oA_o)_{TLV}$ Initial	Ratio, $(A_s\text{-}V_oA_o)_{TLV}$ Steady-state	Ratio, $(A_s\text{-}V_oA_o)_{IDLH}$ Initial	Ratio, $(A_s\text{-}V_oA_o)_{IDLH}$ Steady-state
BRATTICE CLOTH				
A	0.020	0.147	0.39	2.96
B	.017	.040	.34	.80
C	.009	.047	.17	.96
D	.008	.055	.17	1.10
E	.032	.056	.66	1.11
F	.058	.537	1.17	10.10
G	.019	.177	.38	3.55
H	.055	.181	1.10	3.63
I	.037	.147	.76	2.96
CONVEYOR BELTING				
P1	0.029	0.043	0.60	0.95
P1A	.033	.044	.71	.99
P2	.039	.036	.84	.78
P3	.024	.039	.50	.83
P4	.046	.066	.97	1.45
P8	.026	.040	.56	.89
SBR	.112	.172	2.38	3.80
NP	.036	.048	.73	1.00

Table 8.—Initial smoke characteristics from smoldering brattice cloth and conveyor belting

Sample	N_o, 10^6 p/cm³	M_o, mg/m³	d_m, μm	d_{32}, μm	Obscuration, pct	OD, m⁻¹
BRATTICE CLOTH						
A	1.27	24.7	0.29	ND	3.0	0.3
B	1.49	67.7	.40	0.39	13.8	1.5
C	1.89	30.9	.28	.37	11.2	1.2
D	1.53	55.0	.37	.49	10.4	1.2
E	1.23	68.4	.42	.35	12.0	1.3
F	1.57	16.8	.25	ND	4.5	.5
G	.92	51.6	.43	.42	8.0	.9
H	1.01	34.1	.37	ND	2.3	.2
I	1.45	30.3	.30	ND	7.3	.8
Jute ...	.36	6.9	.29	ND	2.6	.3
CONVEYOR BELTING						
P1	0.52	156.5	0.75	0.58	15.8	1.5
P1A ...	.87	164.5	.77	.54	15.7	1.7
P2	.52	116.6	.68	.57	17.1	1.8
P3	1.35	149.7	.55	.44	15.4	1.7
P4	.50	74.9	.58	.52	13.0	1.4
P8	.78	107.9	.51	.58	19.9	2.2
SBR ...	.63	51.3	.47	.50	10.4	1.1
NP	1.49	47.6	.36	.21	9.9	1.0

ND   Not determined.

Table 9.—Steady-state smoke characteristics from smoldering brattice cloth and conveyor belting

Sample	N_o, 10^6 p/cm³	M_o, mg/m³	d_m, μm	d_{32}, μm	Obscuration, pct	OD, m⁻¹
BRATTICE CLOTH						
A	0.82	2.7	0.15	ND	3.0	0.3
B	1.07	3.5	.14	ND	13.8	1.5
C	1.32	4.9	.17	ND	11.2	1.2
D	1.16	8.2	.21	ND	10.4	1.2
E	1.24	8.5	.21	0.33	12.0	1.3
F	1.55	3.2	.14	ND	4.5	.5
G	.74	3.1	.16	.33	8.0	.9
H	.91	5.2	.19	ND	2.3	.2
I	.88	4.7	.20	ND	7.3	.8
Jute ...	.39	.8	.14	ND	.4	<.1
CONVEYOR BELTING						
P1	0.74	68.0	0.49	0.48	13.3	1.4
P1A ...	.60	70.9	.55	.44	12.2	1.2
P2	.70	25.1	.34	.46	12.7	1.4
P3	1.57	69.4	.39	.35	12.5	1.3
P4	.32	55.7	.64	.51	16.3	1.6
P8	.69	18.0	.31	.54	17.3	1.8
SBR ...	.49	34.4	.42	.37	8.6	.9
NP	1.54	40.7	.33	ND	7.0	.8

ND   Not determined.

DETECTION LIMITS

Smoldering materials that do not produce much smoke or toxic gas are less hazardous, but are also more difficult to detect. This can be demonstrated by calculating the CO_A (equation 8) and OD_A (equation 12) for smoldering brattice cloths and conveyor belts. Tables 10 and 11 list these values for the initial stage and steady-state stage. The lowest set point for a CO sensor to safely detect smoldering brattice cloths is below the alarm threshold of most CO sensors (5 ppm). Smoldering conveyor belts are easier to detect and require slightly higher thresholds.

In a similar manner, the CO_A and OD_A at the IDLH level would be required to warn of extremely unsafe conditions. Figures 6 and 7 illustrate the effectiveness of sensors with specific threshold alarm levels. The nontoxic region would have a relative hazard level below the TLV. In this area, smoke detection for all belts and most brattices is effective. The potentially toxic region would have a relative hazard between the TLV and IDLH level. CO detection for some belts and all brattices lie in this area. Only smoldering brattices A, C, and D could not be detected in the nontoxic region by a 0.1-m^{-1} smoke sensor. Only smoldering belts P3 and NP could not be detected in the nontoxic region by a 5 ppm CO sensor. The combustion emissions from these belts may be less toxic, but more difficult to detect. Figures 6 and 7 confirm that smoke detection is more effective than CO detection. It is also clear that smoldering conveyor belts are more detectable than smoldering PVC brattice cloths.

Table 10.—Minimum requirements for sensor alarm thresholds from initial stage

Sample	CO_A, ppm		OD_A, m^{-1}	
	at TLV	at IDLH	at TLV	at IDLH
BRATTICE CLOTH				
A	0.70	14.11	0.049	0.97
B	1.66	33.75	.200	4.06
C	1.18	23.69	.084	1.70
D	.36	7.29	.086	1.72
E	3.31	67.77	.328	6.71
F	1.14	23.00	.254	5.12
G	.70	14.16	.146	2.93
H	.93	18.79	.107	2.15
I	2.02	40.93	.232	4.71
CONVEYOR BELTING				
P1	7.32	153.95	0.345	7.26
P1A ...	11.60	251.23	.461	9.98
P2	10.04	215.30	.580	12.45
P3	3.41	69.70	.332	6.79
P4	7.45	156.51	.504	10.59
P8	8.46	179.55	.445	9.44
SBR ...	8.78	186.51	.912	19.37
NP	3.28	66.95	.277	5.66

Table 11.—Minimum requirements for sensor alarm thresholds from steady-state stage

| Sample	CO_A, ppm		OD_A, m^{-1}	
	at TLV	at IDLH	at TLV	at IDLH
BRATTICE CLOTH				
A	0.62	12.53	0.160	3.21
B	2.02	51.06	.203	5.13
C	2.07	41.99	.200	4.06
D	.33	6.53	.247	4.96
E	.68	13.61	.211	4.25
F	2.60	49.00	1.044	19.64
G	.92	18.45	.590	11.86
H	.53	10.71	.150	3.00
I	1.09	21.86	.393	7.91
CONVEYOR BELTING				
P1	11.41	250.79	0.478	10.51
P1A ...	13.64	305.45	.456	10.21
P2	8.68	186.38	.407	8.74
P3	5.93	124.29	.416	8.72
P4	11.36	249.60	.824	18.11
P8	13.31	297.39	.560	12.52
SBR ...	12.29	272.17	1.198	26.53
NP	5.32	92.20	.336	5.82
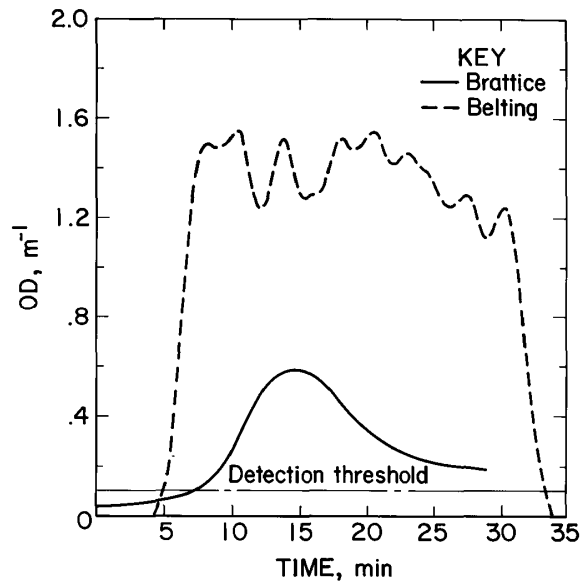
Figure 5.—Results of typical OD levels for PVC brattice and conveyor belting.
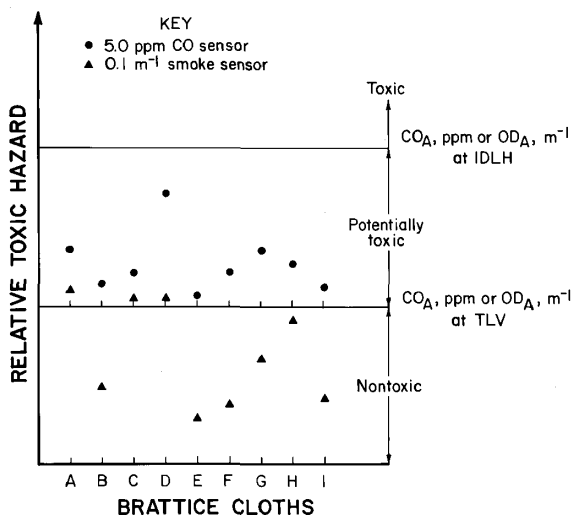
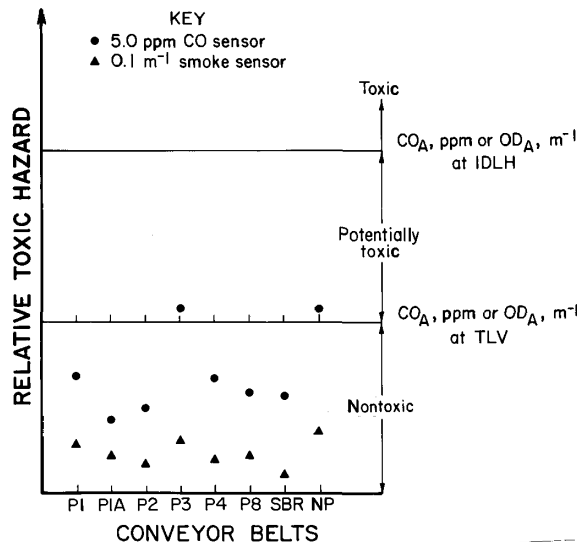Figure 6.—Detection limits for smoldering brattice cloths for initial stage.

Figure 7.—Detection limits for smoldering conveyor belts for initial stage.

COMPARISON OF MATERIALS TESTED

SMOLDERING EMISSIONS

A comparison of the gas concentrations and smoke characteristics of other smoldering combustible mine materials was reported previously (15). This report updates and expands those results. The tests were all conducted in the intermediate-scale fire tunnel and all materials were pyrolyzed using strip heaters. The tables combine the initial stage results from this report with the earlier smoldering data.

A summary of the updated gas concentrations can be found in table 12. Those materials with high gas production, jute brattice, and nonignitable ducting, have higher CO_2-CO ratios indicating more complete combustion. Lower ratios, indicative of less efficient combustion, are usually produced from smoldering fires. PVC brattice, although it has low gas production, has a high CO_2-CO ratio.

A summary of the smoke characteristics is in table 13. The particle size is a major factor in smoke density. Those materials with large particle size tend to produce thick smoke. For example, the particles, d_m and d_{32},

produced from smoldering PVC belts resulted in dense smoke as measured by the obscuration and OD.

Table 12.—Gas concentrations and CO_2-CO ratios from initial stage of smoldering combustion

Material	CO, ppm	CO_2, ppm	Ratio, CO_2-CO
PVC brattice	7	37	6.9
Jute brattice	32	149	4.6
PVC belts	31	31	1.0
SBR belts	10	20	2.0
NP belts	12	24	2.0
Wood	43	ND	ND
Coal	15	19	1.3
Nonignitable ducting	28	139	5.0
ND Not determined.			

DETECTABILITY

To determine which type of fire sensor (smoke or CO) might be more effective for detection of smoldering PVC

brattice and belts, compare figures 3 and 5 for onset of detectable smoke (OD = 0.1 m⁻¹) and CO (5 ppm). The smoke from smoldering PVC conveyor belts reaches the alarm threshold at the 5th min while the smoke from PVC brattice reaches the alarm threshold at the 7th min. The same comparison for CO detection is even more striking. Most brattices did not produce enough CO to reach the alarm threshold, but the PVC belting exceeded the alarm threshold at the 7th min. A comparison of the relative levels of CO and smoke at respective alarm thresholds for initial stage emissions of all the combustibles tested can be found in table 14. A smoke sensor is the obvious choice because the OD of the smoke is well above the alarm threshold by the time the CO threshold is reached. Jute brattice is the only exception with CO detection only slightly ahead of smoke detection. Table 15 ranks mine combustibles for ease of fire detection. The combustion emissions detected by a CO sensor are in reverse order of smoke detection, and that all the combustibles tested are more readily detected by smoke (OD) than by CO production.

Table 15.—Detectability ranking of initial stage from smoldering mine combustibles

Material	CO sensor	Smoke sensor
Jute brattice	1	8
Wood	2	7
Nonignitable ducting	3	6
Coal	4	5
PVC belts	5	4
NP belts	6	3
SBR belts	7	2
PVC brattice	8	1

During the steady-state stage, the levels change slightly as seen in table 16. Jute brattice has surpassed the alarm threshold of CO, but remains just below the smoke alarm threshold. The detectability ranking also changes (table 17) and is not quite in the reverse order for smoke sensors.

Table 13.—Smoke characteristics from initial stage of smoldering combustion

Material	d_m μm	d_{32} μm	Obscuration, pct	OD, m⁻¹
PVC brattice . .	0.35	0.41	8	0.89
Jute brattice . .	.29	ND	3	.30
PVC belts	.64	.54	16	1.94
SBR belts	.47	.50	10	1.06
NP belts	.36	.21	10	1.02
Wood	ND	ND	12	1.36
Coal	.16	ND	9	.91
Nonignitable ducts	.28	.36	11	1.20

ND Not determined.

Table 14.—Relative levels of CO and smoke at respective alarm thresholds from initial stage of smoldering fires

Material	OD, 15 ppm CO	CO, 0.1 m⁻¹ OD
PVC brattice	0.6	0.8
Jute brattice	<.1	10.6
PVC belts	.3	1.6
SBR belts	.5	1.0
NP belts	.4	1.2
Wood	.2	3.2
Coal	.3	1.7
Nonignitable ducting	.2	2.3

Table 16.—Relative levels of CO and smoke at respective alarm thresholds of steady-state stage from smoldering fires

Material	OD, 15 ppm CO	CO, 0.1 m⁻¹ OD
PVC brattice	1.0	0.5
Jute brattice	<.1	16.0
PVC belts	.4	.7
SBR belts	.9	1.0
NP belts	.3	1.6
Wood	.3	3.2
Coal	.6	1.7
Nonignitable ducting	.4	2.3

Table 17.—Detectability ranking of steady-state stage from smoldering mine combustibles

Material	CO sensor	Smoke sensor
Jute brattice	1	8
Wood	2	7
NP belts	3	4
Nonignitable ducting	4	6
PVC belts	5	2
Coal	6	5
SBR belts	7	3
PVC brattice	8	1

CONCLUSIONS

In a mine fire, all the burning materials combine to produce a wide variety of toxic or irritating gases and particles that can be transported by the ventilating system. Previous studies have identified and measured the products of PVC combustion (*16*). These toxic emissions may overcome their victims far removed from the actual fire. More effective sensing devices and smoke alarms would alert miners of dangerous situations while there is adequate time to take appropriate action.

Smoldering jute brattice will alarm a 5 ppm CO sensor before a smoke sensor. At the other end of the spectrum, a smoke sensor is the more efficient method of detecting smoldering PVC brattice. PVC brattice also had the highest CO_2-CO and HCl-CO ratios. The combustion of these small samples has demonstrated the potential for smoldering PVC brattices to produce toxic smoke levels before detection by most CO sensors. Smoldering conveyor belts are, by comparison, more detectable. However, smoke detectors are still more effective than CO sensors. The irony of the toxicity-detectability dilemma is that the materials producing low toxic emissions may be less detectable. Fires involving these materials may smolder for a long period before emissions reach alarm thresholds levels. Therefore, emissions containing low smoke and CO concentrations could be considered less toxic, but still hazardous because they are more difficult to detect.

It was not the intent of these experiments to judge which material is the most hazardous. Each generates unique and dangerous combustion products. The pyrolysis of synthetic materials adds small, volatile, organic compounds which are highly flammable to the toxic CO, increasing the hazards of their emission products. In any fire, as fresh materials are engulfed the composition of the emissions changes. To determine the total toxicity of the mixture, the possible synergistic effect of the thermal decomposition and combustion products must be considered. In this series of experiments, each material was studied independently to compare their combustion product emission rates, relative toxicities, and the detectability of their toxic products.

REFERENCES

1. Egan, M. R., and C. D. Litton. Wood Crib Fires in a Ventilated Tunnel. BuMines RI 9045, 1986, 18 pp.

2. Egan, M. R. Transformer Fluid Fires in a Ventilated Tunnel. BuMines IC 9117, 1986, 13 pp.

3. ____. Coal Combustion in a Ventilated Tunnel. BuMines IC 9169, 1987, 13 pp.

4. ____. Emission Products from the Combustion of Conveyor Belts. BuMines IC 9205, 1988, 12 pp.

5. ____. Thermal Decomposition of Ventilation Ducting. BuMines IC 9263, 1990, 12 pp.

6. McCaffrey, B. J., and G. Heskestad. A Robust Bidirectional Low-Velocity Probe for Flame and Fire Application. Combust. and Flame, v. 26, No. 1, 1976, pp. 125-127.

7. Patashnick, H., and G. Rupprecht. Microweighing Goes On-Line in Real Time. Res. and Dev., v. 28, No. 6, 1986, pp. 74-78.

8. Cashdollar, K. L., C. K. Lee, and J. M. Singer. Three-Wavelength Light Transmission Technique To Measure Smoke Particle Size and Concentration. Appl. Optics, v. 18, No. 11, 1979, pp. 1763-1769.

9. Hilado, C. J. (ed.). Flammability Handbook for Plastics. Technomic Publ., 3d ed., 1982, pp. 56-59.

10. Parmeggiani, L. (ed.). Encyclopedia of Occupational Health and Safety. Int. Labour Organ., v. 1, 3d ed., 1983, p. 395.

11. Parmeggiani, L. (ed.). Encyclopedia of Occupational Health and Safety. Int. Labour Organ., v. 1, 3d ed., 1983, p. 1084.

12. Hartzell, G. E., A. F. Grand, and W. G. Switzer. Modeling of Toxicological Effects of Fire Gases: VI. Further Studies on the Toxicity of Smoke Containing Hydrogen Chloride. J. Fire Sci., v. 5, No. 6, 1987, pp. 368-391.

13. American Conference of Governmental Industrial Hygienists. Threshold Limit Values for Chemical Substances and Physical Agents in the Workroom Environment with Changes. 1980, pp. 1-93.

14. Tewarson, A., and J. S. Newman. An Experimental Investigation of the Fire Hazards Associated With Timber Sets in Mines. Paper in Underground Metal and Nonmetal Fire Protection. BuMines IC 8865, 1981, pp. 86-103.

15. Egan, M. R. Summary of Combustion Products from Mine Materials: Their Relevance to Mine Fire Detection. BuMines IC 9272, 1990, 12 pp.

16. Ultrasystems, Inc. Coal Mine Combustion Products Identification and Analysis Procedures and Summary (contract H0133004), 1978, 130 pp.

APPENDIX.—SYMBOLS USED IN THIS REPORT

A_X	area of a given material, m^2
CO_A	minimum requirement for CO sensor alarm threshold, ppm
d_m	diameter of a particle of average mass, μm
d_{32}	surface mean particle size, μm
$\dot{G}_X$	generation rate of a given combustion product, g/s
$\dot{G}'_X$	generation rate of a given combustion product from a given area of sample, $g/(m^2 \cdot s)$
ℓ	path length, m
ln	logarithm, natural
M_o	particle mass concentration, mg/cm^3
M_X	density of a given gas, $g/(m^3 \cdot ppm)$
N_o	particle number concentration, p/cm^3
OD	optical density, m^{-1}
OD_A	minimum requirement for smoke sensor alarm threshold, m^{-1}
p	particle
T	transmission of light
$V_o A_o$	ventilation rate, m^3/s
Δm	measured change in mass, g
ΔX	measured quantity of a given gas, ppm
λ	wavelength of light source, μm
ρ_p	individual particle density, g/cm^3